Quantifying the Puncture Resistance of Optical Fiber Coatings

G. Scott Glaesemann and Donald A. Clark

Corning Incorporated
Corning, New York
+1-607-974-3736 · glaesemags@corning.com

Abstract

A simple puncture resistance test has been developed to quantify the ability of fiber coatings to protect the underlying glass surface. Fibers with a wide range of coated dimensions were examined with this test method. Fibers without primary coating were included in the testing as well as fiber with a variety of glass dimensions. Puncture resistance was found to depend linearly on the cross-sectional area of the secondary coating regardless of glass diameter or the presence of primary coating. This understanding is important for the designing of fiber handling processes and the design of both glass and coating for special applications.

Keywords

Optical Fiber; Mechanical Reliability; Damage

1. Introduction

One of the most persistent failure modes for optical fiber is glass damage through the protective polymer coating during fiber processing and handling. Fiber with today's standard coating dimensions can be handled without damaging the coating; however, it is necessary to regularly clean and maintain pulleys and rollers that contact the fiber. With the advent of photonic devices fibers are handled significantly more than in cabling and coating damage resulting in fiber breaks can be a significant cost of manufacturing.

The ability of protective optical fiber coatings to resist damage to the underlying glass is not well understood. One test strategy has been to damage the coating surface with an increasingly abrasive surface until the glass is damaged. In 1993 Oishi et al. [1] published a test method whereby fiber in tension is passed over a roller covered with sandpaper. A schematic of this test method is shown in Figure 1. Coating thickness is plotted versus the grit size of the sandpaper in Figure 2. They concluded that particle sizes greater than twice the secondary coating thickness cause the fiber to break in this test.
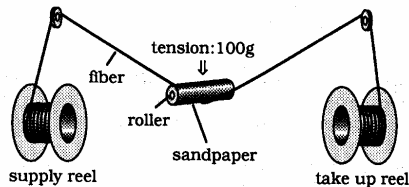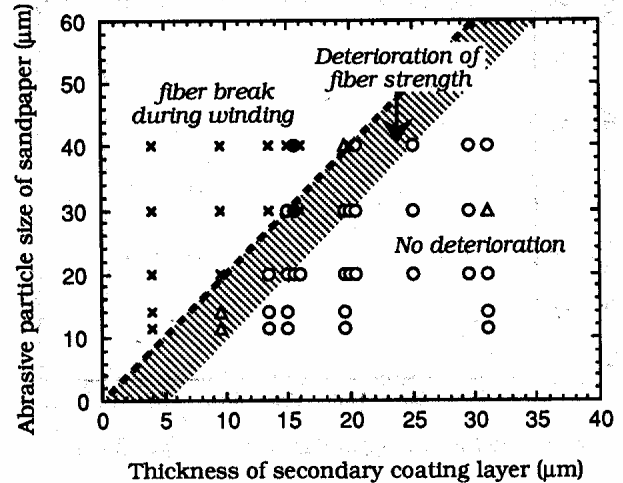

Figure 1. Oishi et al. abrasion test.[1]

Figure 2. Dependence of secondary coating thickness on abrasive particle size.[1]

This test method was also used by Kobayashi et al. in 1995.[2] Note that too few details are given in the description of this test method to evaluate its variability and reproducibility. For example, some sandpaper manufacturers coat the abrasive with a thin layer of polymer and sometimes the binder wicks over the abrasive material. Furthermore, during the test some secondary coating wears away and impregnates the sandpaper, thereby, creating an abrasive surface that changes during the test event. The test is also subject to changing relative humidity and temperature.

In 1994 the "pulse" test was used to evaluate the damage resistance of fibers with a range of coating dimensions.[3] The test strategy here was to use a constant surface roughness and to increase the lateral load of the fiber against that surface until the coating ruptured. Fiber was tensioned around a rough aluminum pulley and pulsed to ever increasing loads until the secondary coating fractured. The results, summarized in Figure 3 show good agreement between the threshold load for damage and the cross-sectional area of the coating. Delamination always preceded coating fracture. This test, though crude, was useful at the time in establishing a correlation between coating dimensions and a threshold for coating damage.
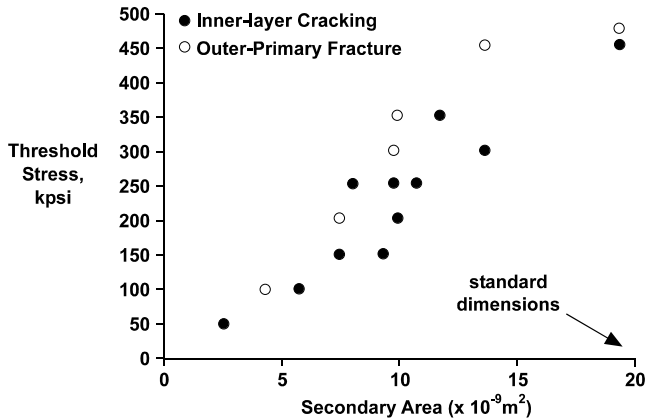
Figure 3. Thresholds for delamination (inner-layer cracking) and secondary fracture using the pulse test.[3].

In 1998 Wissuchek et. al.[4] were able to isolate the fracture energy of secondary coatings using an indentation test directly on coated optical fiber. To our knowledge, this was the first study to quantify the protectability of fiber coatings in fracture energy or fracture toughness terms. A key feature of this test method was the use of two different microhardness indenters. A Vickers diamond pyramid and a diamond wedge indenter, with an included angle of 75°, were driven into the coated fiber resulting in a load drop when the secondary coating ruptured. The schematic of an indented fiber in Figure 4 shows three mechanisms for strain energy absorption: (1) plastic deformation of the secondary coating, (2) fracture of the secondary coating, and (3) fracture of the glass/primary interface.
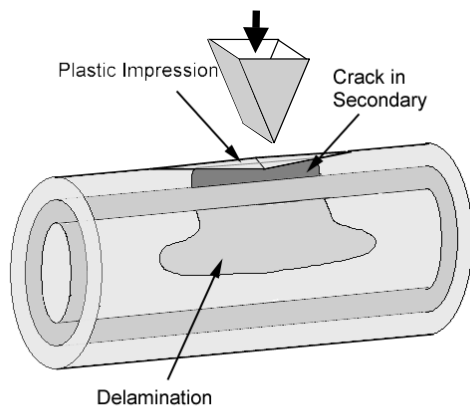

Figure 4. Schematic of coating indentation event.[4]

It was determined that most of the fracture energy went into fracture of the secondary. The fracture energy of delamination was found to be about 15 to 20% of the fracture energy of the secondary. Plasticity of the secondary coating comprised about 1% of the total strain energy. The purpose of this paper is to demonstrate a simplified Wissuchek et. al.[4] test method and its usefulness in quantifying the puncture resistance of fiber coatings.

2. Experimental Method and Procedure

2.1 Indentation Test Method

One of the advantages of using indentation as a means for quantifying puncture resistance of optical fiber coatings is that the object causing the damage is well controlled. Another advantage is that only a few centimeters of fiber are required.

Specimen preparation is as follows. A 4-centimeter length of fiber is placed on a 3 mm-thick glass slide. One end of the fiber is attached to a device that allows one to rotate the fiber in a controlled fashion. This fiber is examined under 100X magnification using transmitted light and is rotated until the secondary coating wall thickness is equivalent on both sides. In this position the secondary coating will be thickest at the top or bottom and equal on the sides. This is shown in exaggerated fashion in Figure 5. This orientation is then fixed by taping the fiber to the slide at both ends. The fiber is now ready for indenting.
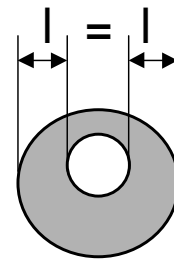

Figure 5. Orienting the fiber for indentation.

Indentation is carried out using an inverted microscope[α] placed beneath the crosshead of a universal-testing machine[β] as shown in Figure 6. The microscope objective was positioned directly beneath a 75° diamond wedge indenter. The glass slide containing the fiber is placed on the moveable microscope stage and positioned directly beneath the indenter such that the width of the wedge is orthogonal to the direction of the fiber. This set-up is shown in Figure 7. Precise positioning is accomplished by lowering the indenter tip into view along with the fiber and then visually aligning the fiber through movement of the slide on the stage.

Figure 6. Testing machine outfitted with inverted microscope for indentation testing.
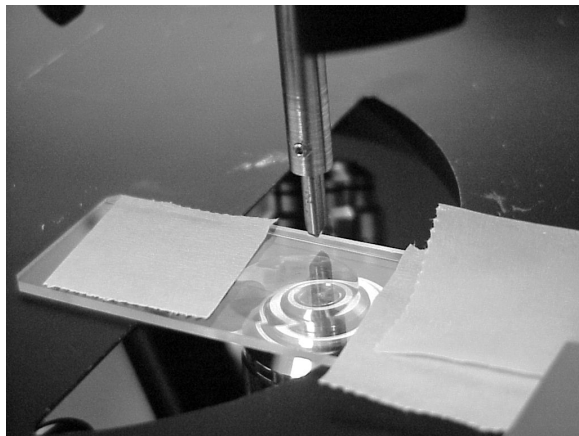

Figure 7. Diamond wedge indenter positioned over microscope slide with attached fiber.

Once the fiber is in place the diamond wedge is lowered until it just touches the coating surface. The wedge is then driven into the coating at a rate of 0.1 mm/min. The load increases until it suddenly drops, signifying that the coating has been punctured. As viewed from the microscope, the drop in load corresponds to visual confirmation that the coating has been punctured. A typical load trace is shown in Figure 8. The peak load at puncture is recorded for ten such measurements and then the fiber is rotated 180° so that the other extreme of the secondary wall thickness can be tested in

the same manner. Thus, twenty measurements are obtained for a given section of fiber.
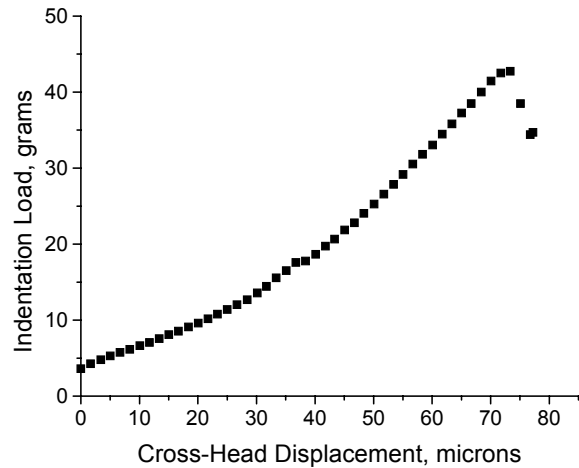

Figure 8. Load increases as wedge indenter presses into the coated fiber until the secondary ruptures at the "puncture load" of 43 grams.

It is important to note that this test method is based on load-to-failure. A similar test could be performed on a displacement basis. That is to say, the net displacement of the wedge indenter at the instant of puncture represents the displacement required for an object puncture through the coating. This may be more pertinent for those processes that contact the fiber with a fixed displacement.

2.2 Coating Dimensions

Coating dimensions are measured on a fiber section within a few centimeters of the punctured section. The specimen is laid in a microscope slide, with a cavity filled with index matching fluid, and placed in a microscope.[δ] A camera is mounted on the microscope and the image is displayed on a high-resolution monitor. Coating dimensions are made using an on-screen measurement system. Calibration is performed using the calibration-slide technique. Due to potential lensing effects of the coatings, the underlying glass diameter of the fiber is also used as a means for calibrating measurements of coated fiber specimens. The glass diameter is obtained from on-draw measurements and the edges of the glass are visually well defined in the optical microscope.

The measurement specimen is rotated until the secondary wall thickness was equal on both sides while looking side-on with transmitted light. The diameter of the primary coating is distinct and easy to measure. The secondary is also measured in this manner; however, this measurement is confounded by difficulty in identifying the edge of the secondary. Thus, all measurements were performed in a self-consistent manner using the same

---

[δ] Nikon Inc., Tokyo, Japan.

technician, microscope, magnification, and camera. It is important to note that the glass diameter measured through the coating in this fashion was identical to that measured on the draw. This provided confidence that the measured coating dimensions were close to the true value. The extreme values for the secondary wall thickness were obtained by simply rotating the fiber 90° from the position where the secondary wall thickness was the same on both sides.

2.3 Fibers

All fibers used in this study were coated with what is standard on Corning fiber. Coating and glass dimensions are given in Table I. Both dual and single coated fibers were created for this experiment. The dual coated fibers were made with 80 and 125 µm glass diameters and the single coated fibers consisted of three glass diameters ranging from 50 to 125 µm.

Table I. Glass and coating dimensions used in this study.

Fiber	Glass Diameter µm	Primary Diameter µm	Secondary Diameter µm
Dual Coat			
A	125	191	244
B	125	195	240
C	125	183	226
D	125	175	207
E	125	169	208
F	125	161	205
G	125	153	188
H	80	145	205
I	80	135	162
J	80	113	164
Single Coat			
K	125	-	245
L	80	-	163
M	52	-	91

3. Results and Discussion
3.1 Puncture Results for a Single Test

The distribution of puncture loads for Fiber A, a fiber with standard dimensions, is shown in Weibull fashion in Figure 9. The thin side of the secondary (triangle) is shown to have a lower puncture load than the thick side (circle). The Weibull modulus, m, for both tests is greater than 25 indicating good reproducibility during a given test. Figure 10 is a contour plot of the Weibull parameters for these two distributions. The distributions are clearly different than one

another, as there is no overlap of the contour lines even to the 95% confidence level.
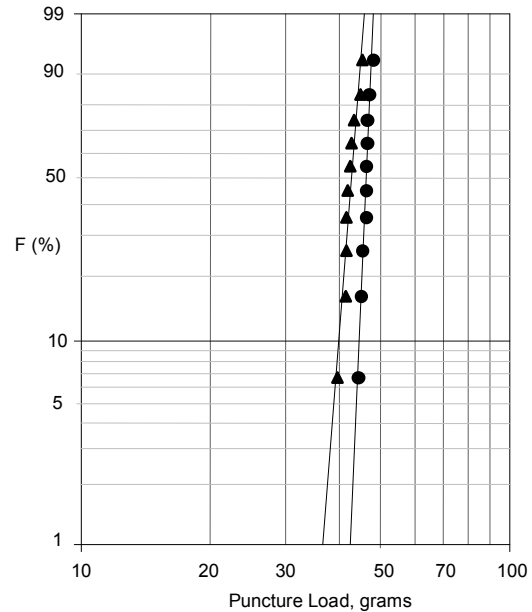

Figure 9. Puncture loads for Fiber A in Table I. The circles are data from the region about the circumference where the coating is thickest and the triangles are where the coating is thinnest.
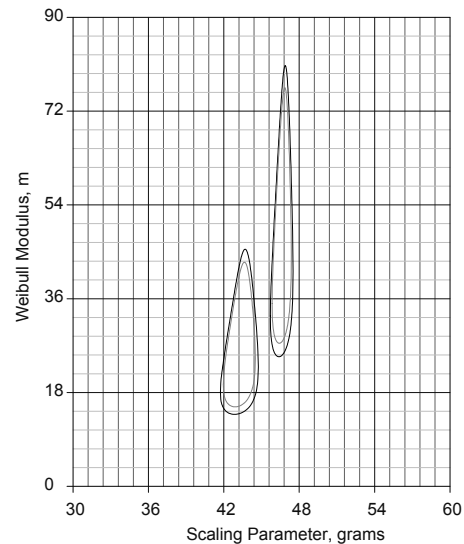

Figure 10. Contour plots of the Weibull parameters for the distributions in Figure 9 show that the distributions are different to the 95% confidence level.   The inner contour line is the 90% confidence interval and the outer the 95% confidence interval.

3.2 Repeatability Study

Fiber A was tested 5 separate times over a span of 7 days to obtain an estimate of test-to-test repeatability of a given fiber's puncture behavior. All 5 tests were conducted on a fiber segment less than 1 meter in length. With each test a small length of fiber was removed from this segment and placed in the test fixture using the procedure given above. Table II contains a summary of the measured fiber dimensions and puncture results. A statistical analysis showed that the results from each test were better described by a normal distribution than a 2-parameter Weibull distribution. The mean puncture load is shown along with 1 standard deviation. For comparison purposes, the corresponding Weibull moduli were all greater than 22. It is clear that a single test yields a "tight" distribution of puncture loads.

Table II. Testing Fiber A five times.

Mean Puncture Load, grams

Test	Thin side	standard deviation	Thick side	standard deviation
1	42.47	1.68	46.14	1.05
2	42.92	1.16	50.63	2.09
3	42.19	1.28	48.37	1.22
4	41.2	1.03	51.47	1.10
5	40.66	1.79	50.02	0.91

The mean values from all five tests seem to be reasonably close together. The maximum difference in means on the thin side is less than 3 grams. On the thick side the maximum difference in means is only 5 grams. A common method for comparing distributions to determine if they are the same or not is the use of contour plots of the confidence limits on statistical parameters, the mean and standard deviation in this case. Contour plots for the thin side is shown in Figure 11. Overlap between contour lines indicates that the distributions cannot be claimed to be different from one another.

3.3 Results From Fibers With Various Glass And Coating Dimensions

A summary of the puncture results is given in Table III for all the fibers in this study. In almost all cases the thicker side of the fiber yielded a higher puncture load; and therefore, one might speculate that there is a correlation between puncture load and secondary wall thickness. The mean puncture load is plotted versus secondary wall thickness in Figure 12 for the fibers in Tables II and III. Note that testing a given length of fiber contributes two data points to the plot. The error bars represent one standard deviation. There is a trend of increasing puncture load with increasing secondary wall thickness; however, the variability in the data suggests a more complex relationship.
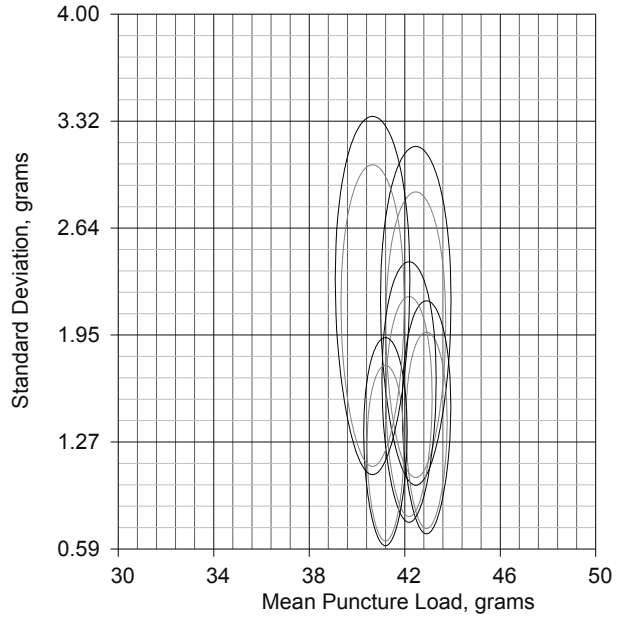

Figure 11. Contour plot of the statistical parameters from the thin side of the repeatability test. The inner contour line is the 90% confidence interval and the outer the 95% confidence interval.
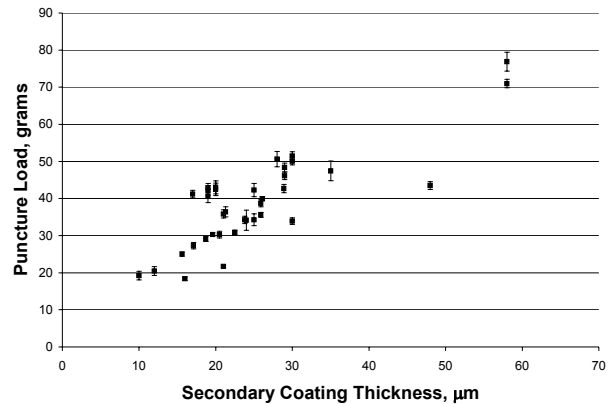

Figure 12. Mean puncture load increases with increasing secondary coating thickness for the fibers in Tables II and III.

Table III. Puncture results for fiber with 50, 80 and 125 micron glass diameters and a range of coating dimensions.

| | Glass Diameter | Primary Diameter | Secondary Diameter | Mean Puncture Load, grams | | | |
| | | | | | | Thick | |
Fiber	μm	μm	μm	Thin side	standard deviation	side	standard deviation
Dual Coat							
A	125	191	244	43.0	1.7	47.5	2.7
B	125	195	240	38.7	0.9	42.7	1.1
C	125	183	226	36.4	1.4	40.0	0.6
D	125	175	207	27.3	0.9	29.1	0.7
E	125	169	208	30.3	0.5	30.2	0.9
F	125	161	205	34.3	1.0	35.6	0.7
G	125	153	188	25.0	0.6	30.8	0.6
H	80	145	205	35.8	1.1	42.3	1.8
I	80	135	162	19.2	1.2	20.5	1.2
J	80	113	164	34.2	2.7	34.3	1.6
Single Coat							
K	125	n/a	245	71.0	1.2	76.9	2.6
L	52	n/a	91	18.40	0.47	21.68	0.38
M	81	n/a	163	33.9	0.9	43.5	1.0

3.4 Hypotheses for Puncture

In this section several failure hypotheses for coating puncture are considered. Note that these hypotheses greatly simplify the complex puncture event. The yield strength is used as the underlying failure criteria. Also, small deflections are assumed, and therefore, creep and plastic deformation are not considered.

3.4.1 Diametrical Compression

The in-situ puncturing of optical fiber coatings begins with the diametrical compression of the secondary coating cylinder. This is prior to any plastic deformation of the coatings or stress concentration due to the shape of the indenter. The maximum stress is located directly beneath the indenter on the inside of the secondary coating, position A in Figure 13.

The hoop stress at point A is given by ,[5,6]

$$\sigma_\theta = K \frac{P}{\pi r_o t} \qquad (1)$$

where the stress concentration factor K is only a function of the ratio r_i / r_o , t is the width of the cylinder and taken to be unity. Assuming the failure criteria for the secondary to be the point at which the stress at A reaches the yield stress of the secondary coating, $\sigma_\theta = \sigma_y$, Eq.(2) becomes,

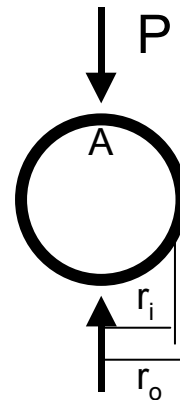$$P = \frac{r_o}{K} \pi t \sigma_y \qquad (2)$$

Figure 13. Schematic of a cylinder under diametrical compression.

Since the yield stress is relatively constant for a given loading condition, the load at failure, P, is a function of the outer radius of the secondary cylinder and the stress concentration factor. Thus, if coating puncture were governed by exceeding the yield stress at point A, then one would expect the measured puncture load, P, to correlate with the dimensional ratio r_o/K. Figure 14 shows that there is no such correlation for data in this study. Either the underlying

failure criterion is incorrect and/or the hypothesis that stress concentration due to diametrical compression is responsible for puncture is suspect.   One reason may be that this hypothesis assumes no influence from the primary coating and underlying glass on the puncture behavior.
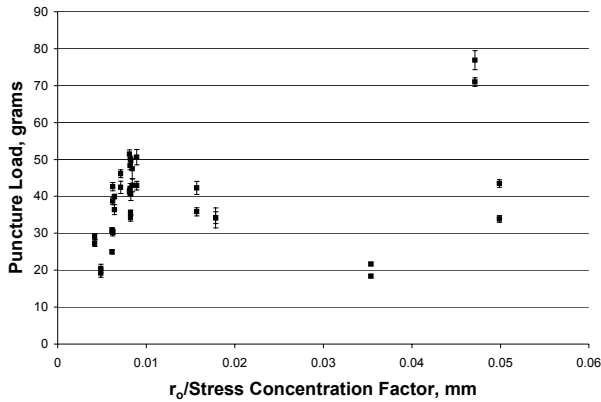

Figure 14. Mean puncture load plotted versus the stress concentration factor for a cylinder in diametrical compression.

3.4.2 Local Deformation of a Thin-Walled Pressure Vessel

In this hypothesis the secondary coating is treated as a circular membrane subjected to a concentrated load. A point load on a thin-walled pressure vessel, shown schematically in Figure 15, generates the hoop stress,[7]

$$\sigma_\theta = C_1 \frac{P}{(r_o - r_i)^2} \qquad (3)$$

where C_1 is a constant. This analysis is bounded by $t/R < 0.1$. Even though the coating configurations examined in this study exceed this condition it is still worthy of consideration.
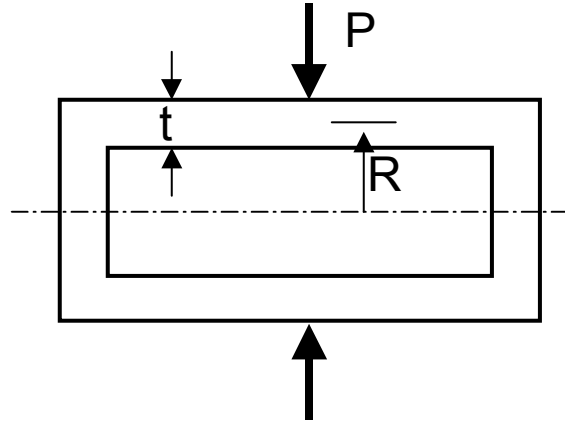

Figure 15. Side-on view of a thin walled pressure vessel subjected to a point load.

For failure, P is proportional to the square of the coating thickness,

$$P = \frac{1}{C_1} \sigma_y (r_o - r_i)^2 \qquad (4)$$

Puncture load is plotted versus thickness squared in Figure 16 for all fibers and Figure 17 for just the dual coated fibers. There is a clear trend in Figure 17 for dual-coated fibers with puncture load increasing with increasing thickness^2. Despite the fact that the coating cylinders in this study do not qualify as thin membranes, this hypothesis deserves further consideration as it has the attractive feature of a concentrated load on a cylindrical vessel. However, the cylinder is not filled and this observation forms the basis of the next failure hypothesis.
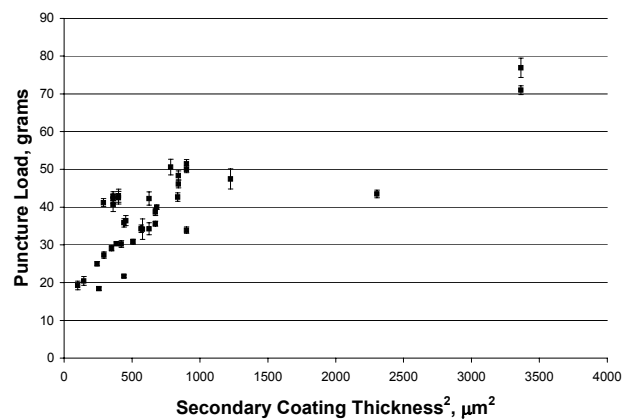

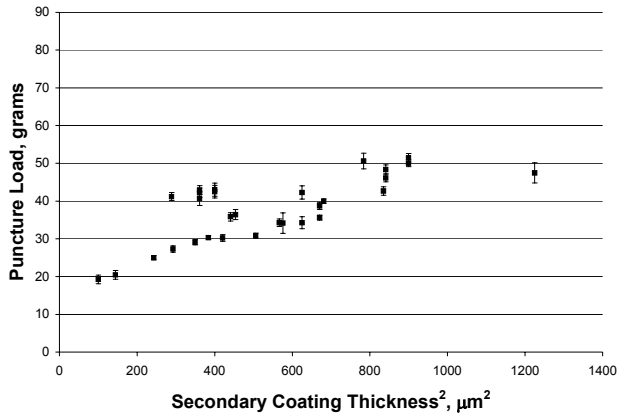**Figure 16. Puncture load versus thickness^2 for all fibers.**

Figure 17. Puncture load versus thickness^2 for just the dual coated fibers.

Figure 18. The dependence of puncture load on cross-sectional area of the secondary coating.

3.4.3 Internal Pressure

Lateral deformation of the cylinder of secondary coating will attempt to reduce the volume of primary coating, thereby, creating hydrostatic pressure in the primary coating. Again, this is assuming small deflections. The pressure of the primary on the inner wall of the secondary coating produces tension in the hoop direction. The maximum hoop stress is at the inner surface of the secondary coating and in the simple case of a cylinder under hydrostatic pressure is [8]

$$\sigma_\theta = \frac{r_o^2 + r_i^2}{A_S}\pi p' \qquad (5)$$

where A_S is the cross-sectional area of the cylinder of secondary coating and p' is the pressure exerted by the primary coating on the secondary. The pressure, p', is directly related to the externally applied load, P. Defining failure again as $\sigma_\theta = \sigma_y$, the applied load is

$$P = A_S \chi(r_o, r_i, E_i/E_o)\sigma_y \qquad (6)$$

where χ is a function of coating properties and dimensions. The point here is that the external force depends on, among other dimensions and properties, the cross-sectional area of the cylinder of secondary coating. Figure 18 shows a strong correlation between puncture load and cross-sectional area of the secondary coating. This correlation is interesting given the fact that the data includes a wide variety of coating dimensions, three different glass diameters, and fibers with dual and single coating layers. This hypothesis is not intuitive for single-coated fiber as there is no low modulus material to produce the needed pressure.
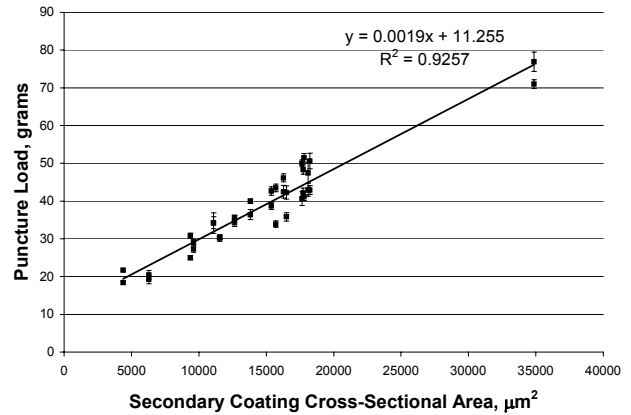
In light of these results the theoretical treatment of a stress generated in a filled cylinder under lateral load, alluded to in Eq. (6), is worthy of further development. This could be approached using either FEA or the superposition of diametrical compression and a vessel under internal pressure. At the very least, Figure 18 can be used as a predictive tool. Relative puncture resistance can be predicted from a known fiber. Other coating compositions are expected to follow a similar trend.

4. Summary

An indentation test method for quantifying the puncture resistance of coatings on optical fiber was used to examine the ability of coatings to protect the underlying glass surface. It was found that the threshold load for puncture correlates well with the cross-sectional area of the secondary. The underlying model is one of increasing hydrostatic pressure in the primary coating during the contact event creating tensile stress in the hoop direction in the secondary coating. Failure is defined as the stress equal to the yield stress of the secondary coating. The correlation between puncture load and cross-sectional area of the secondary coating is independent of glass diameter and coating configuration (dual or single coat). Despite the immaturity of the underlying mechanics model, one can use this dependence to predict the effect of coating dimensional changes on puncture resistance.

Acknowledgments

The authors appreciate the helpful guidance of John Helfinstine.

References

[1] K. Oishi, W. Katsurashima, T. Kakuta, Y. Matsuda, and S. Tanaka, "Coating Design of Thin Coated Fiber for Ultra-High-Count Optical Fiber Cable," pp. 687-693, IWCS proceedings, 1993.

[2] K. Kobayashi, N. Okada, K Mitsuhashi, K. Ishida, M. Miyamoto, and S. Araki, "Coating Design of Thin-Coated Ribbons using 259μm Coated Fibers," pp. 607-615, IWCS proceedings, 1995.

[3] G.S. Glaesemann, "Process Handleability of Thin-Coated Optical Fibers," OFC'94 Tech. Digest, **5**, 243-244 (1994).

[4] D.J. Wissuchek, D.J. Walter, D.A. Clark, and G.S. Glaesemann "Fracture and Abrasion Resistance Test for Optical Fiber Coatings," pp. 309-314, Mat. Res. Soc. Symp. Proc. Vol. 531, 1998.

[5] A.J. Durelli and Y.H. Lin, "Stresses and Displacements on the Bountaries of Circular Rings Diametrically Loaded," J. Appl. Mech., **53** [3] 213-219 (1986).

[6] M. Batista and J. Usenik, "Stresses in a Circular Ring under Two Forces Acting along a Diameter," J. Strain Analysis, **31** [1] 75-78 (1996).

[7] Roark's Formulas for Stress and Strain, 6th Edition, McGraw-Hill, New York, 1989.

[8] O.M. Jadaan, D.L. Shelleman, J.C. Conway, J.J. Mecholsky, Jr., and R.E. Tressler, "Prediction of the Strength of Ceramic Compenents: Part 1 – Analysis," J. Testing and Evaluation, **19** [3] 181-191 (1991).
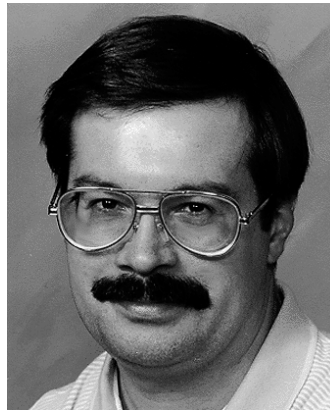
G. Scott Glaesemann

SP-DV-01-7
Corning Incorporated
Corning, NY 14831

Scott Glaesemann is a Sr. Development Associate responsible for the optical fiber mechanical testing laboratory at Corning's Sullivan Park Technology Center. He received his Master's degree and doctorate in mechanical engineering from the University of Massachusetts and a bachelor's degree in mechanical engineering from North Dakota State University.

Donald A. Clark

SP-BN-01
Corning Incorporated
Corning, NY 14831

Don Clark is a Sr. Development Technician in the mechanical testing laboratory for optical fiber at Corning's Sullivan Park Technology Center. His responsibilities include developing new strength and fatigue test techniques as well as performing mechanical reliability studies on commercial and developmental fibers. Clark joined Corning in 1992.